SLAC-PUB-8743
December, 2000

Surface Roughness Impedance*

G. V. Stupakov
Stanford Linear Accelerator Center, Stanford University, Stanford, CA 94309

Abstract

The next generation of linac-based free electron lasers will use very short bunches with a large peak current. For such beams, the impedance caused by submicron imperfections in the vacuum beam tube may generate an additional energy spread within the bunch. A review of two mechanisms of the roughness impedance is given with the emphasis on the importance of the high-aspect ratio property of the real surface roughness.

Presented at ICFA Beam Dynamics Workshop on Physics of and Science with X-Ray Free Electron Laser, 11-15 Sep. 2000, Arcidosso, Italy

*Work supported by Department of Energy contract DE–AC03–76SF00515.

Surface Roughness Impedance

G. V. Stupakov

Stanford Linear Accelerator Center Stanford University, Stanford, CA 94309

Abstract. The next generation of linac-based free electron lasers will use very short bunches with a large peak current. For such beams, the impedance caused by submicron imperfections in the vacuum beam tube may generate an additional energy spread within the bunch. A review of two mechanisms of the roughness impedance is given with the emphasis on the importance of the high-aspect ratio property of the real surface roughness.

INTRODUCTION

The design of modern free-electron lasers based on self-amplified spontaneous emission (SASE) calls for intense short electron beams with a small relative energy spread [1,2]. For example, in the Linear Coherent Light Source (LCLS) at SLAC the peak current is 3.4 kA, the rms bunch length is 20 microns, and the energy spread is less than 0.1 %. A combination of a high current and a short bunch length raises a concern that the induced wakefields may increase the energy spread beyond the tolerable level. It has been pointed out in [3,4] that a major source of wakefields might be the roughness of the surface of the beam pipe in the FEL undulator.

In the first model of wakefields [3] the roughness was simulated by a collection of bumps of a given shape randomly distributed over a smooth surface. If the bump dimensions are small compared to the bunch length, the impedance in this model is purely inductive. For such simple shapes of the bumps as hemispheres or cubes, the model predicts relatively large impedance and results in severe tolerances on the level of roughness.

A more realistic model of roughness effects was developed in Ref. [5]. In this model, the rough surface is considered as a terrain with a slowly varying slope. As was shown in direct measurements of the surface roughness with Atomic Force Microscope [6], this representation of the roughness is adequate to the real surface of the prototype pipe for the LCLS undulator. In the limit when the bunch length is larger than the correlation length of the roughness, the impedance in this model is also inductive, however the tolerance on the rms height of the surface roughness are much looser than predicted in [3].

In yet another approach [4], the roughness wakefield was associated with the excitation of a resonant mode whose phase velocity is equal to the speed of light. The existence of such modes in a round pipe with periodically corrugated walls was studied theoretically in Ref. [7]. In the case when the typical depth of the wall perturbations is comparable to the period, it was shown the the loss factor of such modes reaches the theoretically maximal value for the resonant wakefield. However, as was shown in [8], when the height of the periodic wall corrugations becomes smaller than the period, the loss factor for the mode rapidly decreases. We believe that the latter model is more appropriate for the real roughness of a well finished metal surface.

In this paper we will try to present the results of the latest studies of the roughness impedance, with the emphasis on the realistic modeling of the roughness surfaces.

HOW DOES A ROUGH SURFACE LOOK LIKE?

A naive idea of a rough surface as a microscopic mountain country with sharp peaks and deep canyons does not correspond to reality. A metal surface with a good finish more resembles the water surface of a swimming pool in quiet weather. Pictures of scanned surfaces for different type of machining can be found in surface metrology books [9,10]. Most of them are characterized by that the typical peak-to-valley height h of the roughness is much smaller than the spacing between the crests g. The *aspect ratio* g/h can easily exceed a hundred for smooth surfaces. Of course, this ratio is only one of the many statistical characteristics of the surface, but as it turns out, it is the most essential feature for understanding the electromagnetic interaction of the electron beam with the surface.

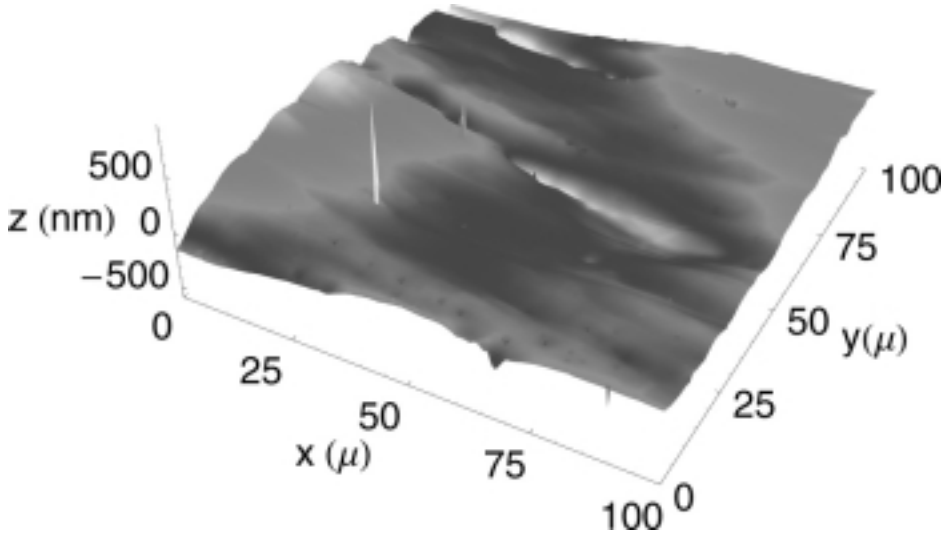

FIGURE 1. A sample surface profile measured with Atomic Force Microscope in Ref. [6]. Note the different scales in the vertical and horizontal directions.

For illustration, we show in Fig. 1 the profile of a surface of a metal pipe measured in Ref. [6]. This pipe is considered as a possible prototype for the vacuum chamber of the LCLS undulator. The rms height of the roughness for this surface is about 100 nm, and the transverse size g, as is seen from the picture, exceeds tens or even a hundred of microns.

SMALL-ANGLE APPROXIMATION IN THE THEORY OF IMPEDANCE

The small ratio h/g implies a small angle θ between the tangent to the surface and the horizontal plane. Using the smallness of this parameter it is possible to develop a perturbation theory of electromagnetic interaction of the beam with the surface based on the so called *small-angle* approximation [5]. This approach extends the earlier treatments [11,12] of an axisymmetric periodic perturbation of the boundary. It also agrees with the more general results of Ref. [13] valid for nonperiodic axisymmetric boundary perturbations.

As follows from Refs. [11,12], for a periodically corrugated wall with the wavelength λ_0 much smaller than the pipe radius b, there exist synchronous modes in the pipe which propagate with the phase velocity equal to the speed of light. The wavelength of these modes is below $2\lambda_0$, so that only a short bunch of length $\sigma_z \lesssim 2\lambda_0$ can efficiently excite these modes. If, on the other hand, the bunch length is larger than λ_0, the excitation of these modes will be exponentially weak. In the roughness problem the parameter g plays the rope of λ_0, and we expect two different regimes depending on whether σ_z is larger or smaller than g.

Long-Bunch Limit, $\sigma_z > g$

In this regime we expect an inductive impedance, because, as explained above, the beam does not lose energy for excitation of the synchronous modes. However, the energy exchange between the head and the tail of the bunch can cause the energy variation along the bunch and may interfere with the lasing.

Let $h(x,z)$ denote the local height of the rough surface as a function of coordinate x in azimuthal direction, and coordinate z along the axis of the pipe (see Fig. 2). The requirement $h \ll g$ can alternatively be expressed as $\theta \approx |\nabla h| \ll 1$. The treatment of Ref. [5] was additionally limited by the assumption that the bunch length is larger than the typical size of the roughness bumps, $\lambda\!\!\!^{-} \sim \sigma_z \gg g$. It was found that in this limit the impedance is purely inductive, and the inductance $\mathcal{L}$ per unit length of the pipe is given by the following formula:

$$\mathcal{L} = \frac{Z_0}{2\pi c b} \int_{-\infty}^{\infty} \frac{\kappa_z^2}{\sqrt{\kappa_\theta^2 + \kappa_z^2}} S(\kappa_z, \kappa_\theta) d\kappa_z d\kappa_\theta, \qquad (1)$$

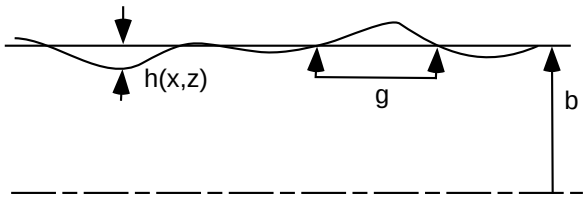

FIGURE 2. The profile of a rough surface. Shown are the height $h(x,z)$, the typical transverse size of the bumps g, and the pipe radius b. Note that the roughness here is not assumed axisymmetric.

where $Z_0 = 4\pi/c = 377$ Ohm, and $S(\kappa_z, \kappa_\theta)$ is the spectrum of the surface profile as a function of wavenumbers k_z and k_θ in the longitudinal and azimuthal directions, respectively. The spectral density S can be defined as a square of the absolute value of Fourier transform of h,

$$S(\kappa_z, \kappa_\theta) = \frac{1}{(2\pi)^2 A} \left| \int_A h(z,x) e^{-i\kappa_z z - i\kappa_\theta x}\, dz dx \right|^2 , \qquad (2)$$

where the integration goes over the surface of a sample of area A. It is assumed that the sample area is large enough so that the characteristic size $\sqrt{A}$ is much smaller than the correlation length g of the roughness.

In Ref. [14] a comparison was done between the small-angle approximation and a previous model of roughness, developed in [3]. It was shown that in the region of mutual applicability both models give the results which, within a numerical factor, agree with each other.

Roughness Measurements

A detailed study of the surface roughness for a prototype of the LCLS undulator pipe using the Atomic Force Microscope was done in Ref. [6]. A high quality Type 316-L stainless steel tubing from the VALEX Corporation with an outer diameter of 6.35 mm and a wall thickness of 0.89 mm with the best commercial finish, A5, was used for the measurements. The samples to be analyzed were cut from this tubing, using an electrical discharge wire cutting process, so as to eliminate damage from mechanical processing. The samples were subsequently cleaned chemically to remove particles adhering to the surface from the cutting process, which used a brass wire.

The measured profiles were Fourier transformed and the inductance $\mathcal{L}$ per unit length of the pipe was calculated using Eq. (1). Because this inductance is inversely proportional to the pipe radius b, a convenient quantity is the product $\mathcal{L}b$ which does not depend on the pipe radius and characterizes the intrinsic properties of the surface. The computed value of this quantity was found to be between 3×10^{-4} pH and 5×10^{-4} pH.

Those values should be compared with the impedance budget for the LCLS beam. For the nominal parameters of LCLS: beam charge 1 nC, $\sigma_z = 20$ μm, undulator length 112 m, and assuming the final beam energy $E = 14.3$ GeV, one finds that the requirement of the relative energy spread $\delta E_{\rm rms}/E$ generated by the wake be less than 0.05% gives the tolerance $\mathcal{L} < 1.6$ pH/m. For the vacuum pipe radius $b = 2.5$ mm the tolerance on the product $\mathcal{L}b$ is $(\mathcal{L}b)_{\rm tol} = 4 \times 10^{-3}$ pH. We see that the measured value of the impedance is almost an order of magnitude smaller than the tolerance.

We have to emphasize here that the above results are based on two assumptions that are not completely fulfilled for the LCLS. First, a Gaussian beam distribution was assumed. As detailed simulations show [1], for the LCLS the bunch shape more resembles a rectangular than a Gaussian shape. Second, Eq. (1) used for the calculation of the inductance, was derived in the limit $\sigma_z \gg g$, which, as roughness measurements indicate, is not satisfied. We will show however, in the next section, that using Eq. (1) in the regime of very short bunches, $\sigma_z < g$, overestimates the impedance, and Eq. (1) can be considered as an upper limit for the real impedance of the roughness.

Arbitrary Bunch Length σ_z

Based on the derivation given in Ref. [5] we will calculate here the wakefield of the roughness which is valid for arbitrary relation between σ_z and g. The corresponding impedance can be used even for large frequencies, when $\lambda < g$. For simplicity, we limit our consideration by the case where the pipe wall has a sinusoidal corrugation, as shown in Fig. 3. The amplitude h_0 of the corrugation is assumed much smaller than the period, $h_0\kappa \ll 1$, which is a requirement of the small-angle approximation. Such a corrugation qualitatively simulates a rough surface with parameter $g \sim \kappa^{-1}$ and the rms height of the bumps of the order of h_0.

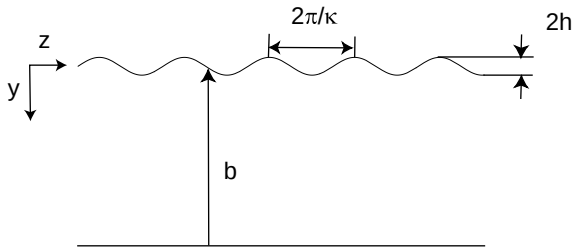

FIGURE 3. A pipe with a sinusoidal corrugation of the wall. The amplitude of the corrugation is h_0, and the period is equal to $2\pi/\kappa$.

The actual derivation of the wake is presented in the Appendix. For the point charge, the longitudinal wake is:

$$w(s) = \frac{h_0^2 \kappa^3}{b} f(\kappa s), \tag{3}$$

where the function f is

$$f(\zeta) = \frac{1}{2\sqrt{\pi}} \frac{\partial}{\partial \zeta} \frac{\cos(\zeta/2) + \sin(\zeta/2)}{\sqrt{\zeta}}. \tag{4}$$

The plot of the function f is shown in Fig. 4. It has a singularity $\sim \zeta^{-3/2}$ when $s \to 0$.

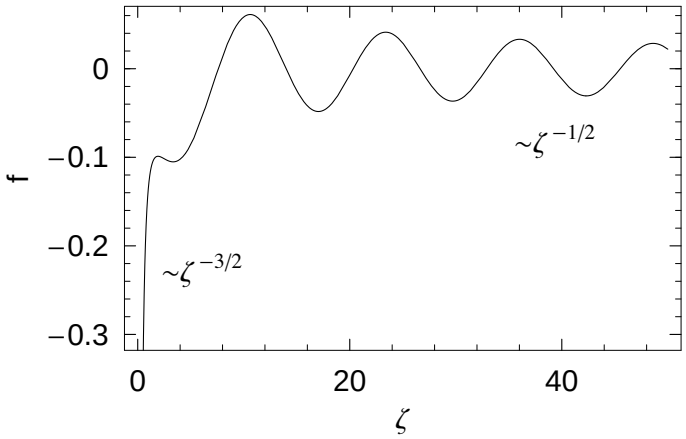

FIGURE 4. The function $f(\zeta)$ for the wake of the sinusoidal corrugation.

To find the wake $W(s)$ for a bunch we need to convolute Eq. (3) with the bunch distribution function $\rho(s)$. For a Gaussian bunch, $\rho(s) = (\sqrt{2\pi}\sigma_z)^{-1} \exp(-s^2/2\sigma_z^2)$, and we have

$$\begin{aligned} W(s) &= \int_s^\infty \rho(s') w(s' - s) ds' \\ &= \frac{h_0^2 \kappa^{3/2}}{b\sigma_z^{3/2}} G\left(\frac{s}{\sigma_z}, \kappa\sigma_z\right), \end{aligned} \tag{5}$$

where the function G for different values of parameters $\kappa\sigma_z$ is shown in Fig. 5.

In the limit of large and small values of $\kappa\sigma_z$ the wake $W(s)$ scales as

$$\begin{aligned} W(s) &\sim \frac{h_0^2 \kappa}{b\sigma_z^2}, \qquad \sigma_z\kappa \gg 1, \\ &\sim \frac{h_0^2 \kappa^{3/2}}{b\sigma_z^{3/2}}, \qquad \sigma_z\kappa \ll 1. \end{aligned} \tag{6}$$

We see from these estimates, that when we use long-bunch approximation ($\sigma_z\kappa \gg 1$) in the regime where $\kappa\sigma_z < 1$, we overestimate the wake by a factor of $(\sigma_z\kappa)^{-1/2} \sim$

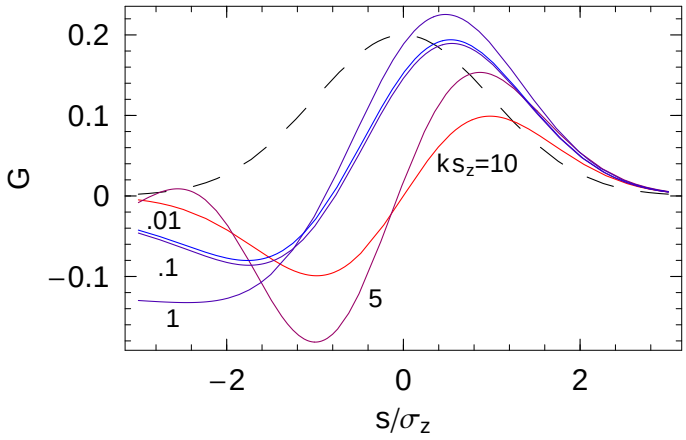

FIGURE 5. The function G for a different values of the parameter $\kappa\sigma_z$ (indicated by numbers on the plot). The dashed curve shows the Gaussian distribution of the beam.

$(g/\sigma_z)^{1/2}$. For this reason, as pointed out at the end of the previous section, the result of Ref. [6] should be considered as an upper boundary for the roughness impedance.

Using Eq. (3) we can also calculate the wake for a rectangular bunch shape, $\rho(s) = 1/l_z$ for $0 < s < l_z$. The result of such calculations for the LCLS is shown in Fig. 6. The parameters used in the calculation are: beam charge 1 nC, $h_0 = 0.28$ μm (corresponding to the rms roughness of 0.2 μm), $g = 2\pi/\kappa = 100$ μm, $L = 112$ m, $E = 14.3$ GeV, $b = 2.5$ mm. The average energy loss for the distribution

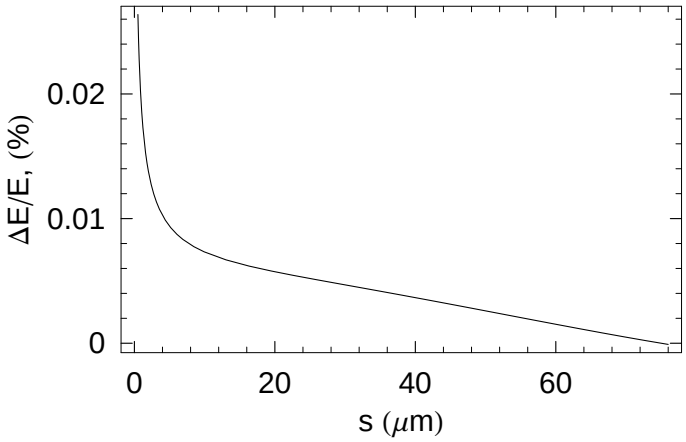

FIGURE 6. The relative energy loss of the LCLS beam at the end of the undulator as a function of position within the bunch.

shown in Fig. 6 is $4.5 \cdot 10^{-3}$ % and the rms energy spread is $2 \cdot 10^{-3}$ %.

SYNCHRONOUS MODE

In addition to the mechanism of the wake generation described in the previous section involving interaction with short-wavelength waves, $\lambda\!\!\!^{-} \lesssim g$, there is another contribution to the wake which was first pointed out by A. Novokhatski and A. Mosnier [4]. It comes from a relatively low-frequency synchronous mode with $\lambda\!\!\!^{-} \gg g$. At first glance, the existence of such mode seems to contradict to the results of Refs. [11,12] which predict that all synchronous modes in a pipe with periodically corrugated surface with the period of corrugation $2\pi/\kappa$ have wavelengths $\lambda\!\!\!^{-} < 2/\kappa$. The answer to this apparent contradiction is that this mode arises in the regime where the perturbation theory of [11,12] is not applicable. As we will show below, in the limit when the amplitude of the corrugation tends to zero, the frequency of this mode increases and approaches the value predicted by the perturbation theory. The contribution of the mode to the wake in this limit becomes negligibly small.

It is interesting to note, that earlier a low-frequency mode in a periodically corrugated waveguide was observed in computer simulations in [15], and also studied theoretically in [16].

Rectangular Corrugations of the Wall

The properties of the synchronous mode in the case of rectangular corrugation of the wall were studied in Ref. [7]. In this paper, the wall roughness was modeled by axisymmetric periodic steps on the surface of height δ, width g, and period p. All three parameters were assumed much smaller than the pipe radius b. The model gives for the frequency ω_0 of the mode

$$\omega_0 = c\sqrt{\frac{2p}{\delta b g}}, \tag{7}$$

and for the longitudinal wakefunction of the point charge

$$w(s) = \frac{Z_0 c}{\pi b^2}\cos(\omega_0 s/c). \tag{8}$$

Surprisingly, the amplitude of the wake in this approximation does not depend on the roughness properties at all. These results however are valid if $kp \ll 1$. We see from Eq. (7) that when δ becomes very small, the parameter k increases and eventually kp becomes comparable to unity. Hence, this model becomes invalid in the limit $\delta \to 0$.

The results of computer simulations that confirm the predictions of this model can be found in Ref. [17,18].

Shallow corrugations

To take into account the effect of the shallowness of the roughness a different model was developed in Ref. [8]. In this model the roughness was treated as a sinusoidal perturbation of the wall shown in Fig. 3 with $h_0\kappa \ll 1$. It was found that, indeed, under certain conditions, a low-frequency synchronous mode with $\lambda\!\!\!^{-}\kappa \gg 1$ can propagate in this system. The longitudinal wake generated by this mode is given by

$$w(s) = \frac{2Z_0 c}{\pi b^2} U \cos(\omega_0 s/c). \tag{9}$$

where the dimensionless factor U and the frequency of the mode ω_0 depend on the parameter $r \equiv h_0\sqrt{b\kappa^3}/2$. The plot of these two functions is shown in Fig. 7. In

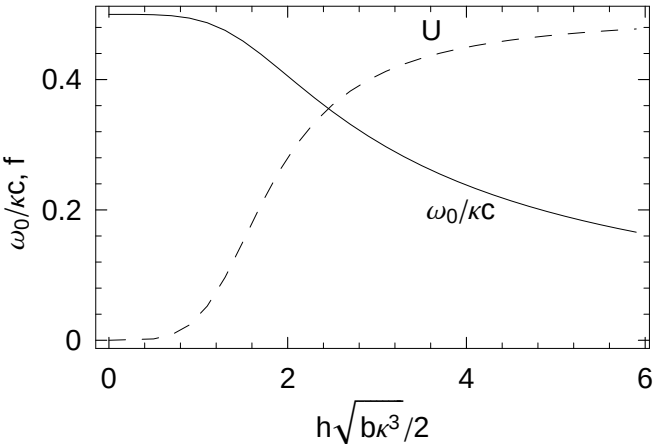

FIGURE 7. Synchronous mode dispersion relation.

the limit $h_0 \to 0$ the frequency ω_0 tends to $\kappa c/2$, and $U \approx r^4/32$. For large values of r, $\omega_0 \approx 2c/h\sqrt{b\kappa}$ and U approaches $1/2$. Interestingly, in this limit we find the amplitude of the wake equal to that in Eq. (7).

Let us estimate the wake for realistic parameters of roughness: $h_0 = 0.28$ μm (corresponding to the RMS roughness of 0.2 μm), $g = 2\pi/\kappa = 100$ μm, and $b = 2.5$ mm. We find $r = h_0\sqrt{b\kappa^3}/2 = 0.11$. The corresponding loss-factor parameter is

$$U \approx 4.5 \cdot 10^{-6}, \tag{10}$$

which indicates that the effect of the wake in this regime will be negligibly small.

CONCLUSIONS

We want to emphasize here that the wakefield generated by the roughness is very sensitive to the geometry of the surface profile. The previous models did not take

into account that the real roughness is typically characterized by the large aspect ratio — the ratio of the characteristic size along the surface (correlation length) and the typical height of the bumps. They overestimated the impedance and lead to the very tight tolerances for the surface smoothness.

The latest models of the roughness predict much smaller impedance. Typical numbers that seem safe for the LCLS undulator are: height ~ 100 nm with $g \sim 100$ μm. The surface measurements [6] shows that these parameters are reasonable for a good surface finish.

ACKNOWLEDGEMENTS

I would like to thank K. Bane and A. Novokhatsky for useful discussions.

This work was supported by Department of Energy contract DE-AC03-76SF00515.

APPENDIX

We write the longitudinal impedance due to roughness as a sum of Eqs. (36) and (43) from Ref. [5]:

$$Z_l(\omega) = -\frac{8k\pi i}{cb^2}\sum_{n,m}\left[1+\frac{n^2}{(\nu_{n,m}^2-n^2)}\right]\int_{-\infty}^{\infty} d\lambda \frac{\lambda^2|\hat{s}_n(\lambda)|^2}{(k+\lambda^2)-(k_{n,m}+i0)^2}\,, \qquad \text{(A1)}$$

where $k_{n,m}=\sqrt{k^2-\nu_{n,m}^2/b^2}$, $\nu_{n,m}$ is the mth root of the derivative of the Bessel function J_n', and $\hat{s}_n(\lambda)$ is the Fourier transform of the roughness profile,

$$\hat{s}_n(\lambda) = \frac{1}{(2\pi)^2}\int_{-\infty}^{\infty} dk \int_0^{2\pi} d\theta\, h(z,\theta) e^{i\lambda z + in\theta}\,. \qquad \text{(A2)}$$

In the limit of high frequency, $\omega \gg c/b$, which was used in the derivation of Eq. (A1), the indices $n, m \gg 1$, and $\nu_{n,m} \approx \mu_{n,m}$ where $\mu_{n,m}$ is the mth root of the Bessel function J_n. Furthermore, in this limit $\nu_{n,m} \approx nf(m/n)$, where the function $f(x)$ is defined by the equation $\pi x = \sqrt{f^2-1} - \arccos f^{-1}$. The summation over m and n in Eq. (A1) can be substituted for integration. Introducing new integration variables $k_x = n/b$, $k_z = \lambda$, and f casts the above equation to the following

$$\begin{aligned} Z_l(\omega) = -\frac{8ki}{cb^2}\int dn\, df \frac{f}{\sqrt{f^2-1}} \\ \times \int_{-\infty}^{\infty} d\lambda \frac{n\lambda^2|\hat{s}_n(\lambda)|^2}{(k+\lambda-k_{n,m}-i0)(k+\lambda+k_{n,m}+i0)}\,. \end{aligned} \qquad \text{(A3)}$$

Using the relation

$$\frac{1}{x+i0} = \mathcal{P}\frac{1}{x} - i\pi\delta(x), \tag{A4}$$

where $\mathcal{P}$ stands for the principal part of the integral, we can write the real part of the impedance as

$$\begin{aligned}\mathrm{Re}\, Z_l(\omega) = \frac{4\pi k}{cb^2}\int dk_z\, dk_x\, df \frac{f k_x k_z^2 |\hat{s}(k_x,k_z)|^2}{\sqrt{f^2-1}\sqrt{k^2-f^2k_x^2}} \\ \times\left[\delta(k+k_z-\sqrt{k^2-f^2k_x^2}) + \delta(k+k_z+\sqrt{k^2-f^2k_x^2})\right]\,,\end{aligned} \tag{A5}$$

where we now use the notation $\hat{s}(k_x,k_z)$ for $\hat{s}_n(\lambda)b$. Performing integration over k_x and f gives the following result

$$\mathrm{Re}\, Z_l(\omega) = \frac{4\pi k}{cb^2}\int dk_z\, dk_x \frac{k_z^2|\hat{s}(k_x,k_z)|^2}{\sqrt{-2kk_z-k_z^2-k_x^2}}\,. \tag{A6}$$

In this integral the integration goes over the negative values of k_z such that the expression under the square root is positive. To find the wakefield we use the relation

$$w_l(s) = \frac{2}{\pi}\int_0^\infty \mathrm{Re}\, Z_l(\omega)\cos\left(\frac{\omega s}{c}\right) d\omega \tag{A7}$$

which gives the following result

$$w_l(s) = \frac{4\sqrt{\pi}}{b^2}\int dk_z\, dk_x |k_z|^{3/2}|\hat{s}(k_x,k_z)|^2\tilde{w}(k_x,k_z,s) \tag{A8}$$

where

$$\begin{aligned}\tilde{w} &= \frac{\partial}{\partial s}\frac{1}{\sqrt{s}}\left(\cos qs + \sin qs\right) \\ &= \frac{1}{2s^{3/2}}\left[(2qs-1)\cos qs - (2qs+1)\sin qs\right],\end{aligned} \tag{A9}$$

with $q = (k_x^2+k_z^2)/2|k_z|$.

It is easy to show that for a sinusoidal perturbation of the surface pipe $h = h_0\cos\kappa z$ the corresponding spectrum is

$$|\hat{s}(k_x,k_z)|^2 = \frac{h_0^2 Lb}{8\pi}\delta(\kappa+k_z)\delta(k_x). \tag{A10}$$

Putting Eq. (A10) into Eq. (A8) and performing integration gives Eq. (3).

REFERENCES

1. *Linac Coherent Light Source (LCLS) Design Study Report: The LCSL Design Study Group*, Report SLAC-R-521, SLAC (1998).
2. *A VUV Free Electron Laser at the TESLA Test Facility Linac – Conceptual Design Report*, Report TESLA-FEL 95-03, DESY Hamburg (1995).
3. K. L. F. Bane, C. K. Ng, and A. W. Chao, *Estimate of the impedance due to wall surface roughness*, Report SLAC-PUB-7514, SLAC (1997).
4. A. Novokhatski and A. Mosnier, in *Proceedings of the 1997 Particle Accelerator Conference* (IEEE, Piscataway, NJ, 1997), pp. 1661–1663.
5. G. V. Stupakov, Phys. Rev. ST Accel. Beams **1**, 064401 (1998).
6. G. Stupakov, R. E. Thomson, D. Walz, and R. Carr, Phys. Rev. ST Accel. Beams **2**, 060701 (1999).
7. K. L. F. Bane and A. Novokhatskii, *The Resonator impedance model of surface roughness applied to the LCLS parameters*, Tech. Rep. SLAC-AP-117, SLAC (March 1999).
8. G. V. Stupakov, in T. Roser and S. Y. Zhang, eds., *Workshop on Instabilities of High Intensity Hadron Beams in Rings* (American Institute of Physics, New York, 1999), no. 496 in AIP Conference Proceedings, pp. 341–350.
9. D. J. Whitehouse, *Handbook of Surface Metrology* (IOP Publishing, 1994).
10. K. J. Stout, *Atlas of Machined Surfaces* (Chapman and Hall, 1990).
11. M. Chatard-Moulin and A. Papiernik, IEEE Trans. Nucl. Sci. **26**, 3523 (1979).
12. S. Krinsky, in W. S. Newman, ed., *Proc. International Conference on High-Energy Accelerators, Geneva, 1980*, CERN, European Lab. for Particle Physics (Birkhäuser Verlag, Basel, Switzerland, 1980), p. 576.
13. R. L. Warnock, *An Integro-Algebraic Equation for High Frequency Wake Fields in a Tube with Smoothly Varying Radius*, Report SLAC-PUB-6038, SLAC (1993).
14. K. L. F. Bane and G. V. Stupakov, *Wake of a rough beam wall surface*, Tech. Rep. SLAC-PUB-8023, SLAC (December 1998), presented at International Computational Accelerator Physics Conference (ICAP 98), Monterey, CA, 14-18 Sep 1998.
15. K. L. Bane and R. D. Ruth, *Bellows Wake Fields and Transverse Single Bunch Instabilities in the SSC*, Tech. Rep. SLAC/AP-45, Stanford Linear Accelerator Center, Stanford, CA, USA (October 1985).
16. V. I. Balbekov, *Calculation of the Corrugated Vacuum Chamber Impedance, (in Russian)*, Tech. Rep. IFVE-85-128, Inst. for High Energy Physics, Protvino, Russia (1985).
17. M. Dohlus, H. Schlarb, R. Wanzenberg, R. Lorenz, and T. Kamps, *Estimation of longitudinal wakefield effects in the TESLA-TTF FEL undulator beam pipe and diagnostic section*, Tech. Rep. DESY-TESLA-FEL-98-02, Deutsches Elektronen-Synchrotron, Hamburg, Germany (March 1998).
18. A. Novokhatsky, M. Timm, and T. Weiland, *Single bunch energy spread in the TESLA cryomodule*, Tech. Rep. DESY-TESLA-99-16, Deutsches Elektronen-Synchrotron, Hamburg, Germany (March 1999).